

THE SHAHEWAN RAPAKIVI-TEXTURED GRANITE - QUARTZ MONZONITE PLUTON, QINLING OROGEN, CENTRAL CHINA: MINERAL COMPOSITION AND PETROGENETIC SIGNIFICANCE

XIAOXIA WANG, TAO WANG, ILMARI HAAPALA AND XINXIANG LU

WANG, XIAOXIA, WANG, TAO, HAAPALA, ILMARI and LU, XINXIANG 2002. The Shahewan rapakivi-textured granite – quartz monzonite pluton, Qinling orogen, central China: mineral composition and petrogenetic significance. *Bulletin of the Geological Society of Finland* 74, Parts 1–2, 133–146.

The Mesozoic Shahewan pluton consists of four texturally different types of biotite-hornblende quartz monzonite. In the porphyritic types alkali feldspar occurs as euhedral or ovoidal megacrysts that are often mantled by one or more plagioclase shells, and as smaller grains in the groundmass. Quartz, plagioclase (An_{20–28}), biotite, and hornblende occur as inclusions in the alkali feldspar megacrysts and, more abundantly, in the groundmass. Euhedral quartz crystals in the groundmass are not as common and well developed as in typical rapakivi granite. Compared to typical rapakivi granites, the mafic minerals (biotite and hornblende) are rich in Mg and poor in Fe, and the whole rock is low in Si, K, F, Ga, Zr, LREE, Fe/Mg, and K/Na. The rocks of the Shahewan pluton are thus regarded as rapakivi-textured quartz monzonites and granites but not true rapakivi granites.

Key words: granites, rapakivi, quartz monzonite, alkali feldspar, phenocrysts, geochemistry, mineralogy, Mesozoic, Shahewan, Qinling, China

Xiaoxia Wang: China University of Geosciences, Beijing 100083, China and Department of Natural Resources, Chang'an University, Xi'an 710054, China and Department of Geology, P.O. Box 64, FIN-00014 University of Helsinki, Finland

E-mail: xiaoxiawang@hotmail.com

Tao Wang: Institute of Geology, Chinese Academy of Geological Sciences, Beijing 100037, China

Ilmari Haapala: Department of Geology, P.O. Box 64 FIN-00014, University of Helsinki, Finland

Xinxiang Lu: Geologic Institute of Henan Province, Zhengzhou 450053, China

INTRODUCTION

A group of Mesozoic 212–217 Ma granitoids with plagioclase-mantled alkali feldspar megacrysts are found along a major suture in the Qinling orogenic belt, central China, and constitutes a special granite - quartz monzonite belt (Lu et al. 1996, 1998, 1999, Zhang et al. 1999). The Shahewan granite - quartz monzonite pluton is a typical example of the intrusions of this belt. Although the rocks are different from the typical Proterozoic rapakivi granites both in age and geological setting (see Rämö & Haapala 1995, 1996, Haapala & Rämö 1999), they have some textural features typical of rapakivi granites. A preliminary description on their geological setting, age and geochemistry is presented in earlier papers (Lu et al. 1996, Wang & Lu 1998, Zhang et al. 1999). In this article, we discuss petrography and mineral compositions of the rocks of the Shahewan pluton in order to make

a more detailed comparison to typical rapakivi granites.

GEOLOGICAL SETTING

The Qinling orogenic belt

The NWN-SSE trending Qinling orogenic belt, central China, separates the North China Block from the South China Block (e.g. Mattauer et al. 1985, Meng & Zhang 1999; Fig. 1). This belt has a complex tectonic and magmatic history. Researchers agree that the belt was formed by amalgamation of the North and South China blocks, but different models have been presented for the integration history (see Meng & Zhang 1999). Several investigators have emphasized the role of Paleozoic collision of the two blocks along the Shangdan suture in formation of the Qinling belt and its Paleozoic-Mesozoic igneous suites (e.g.

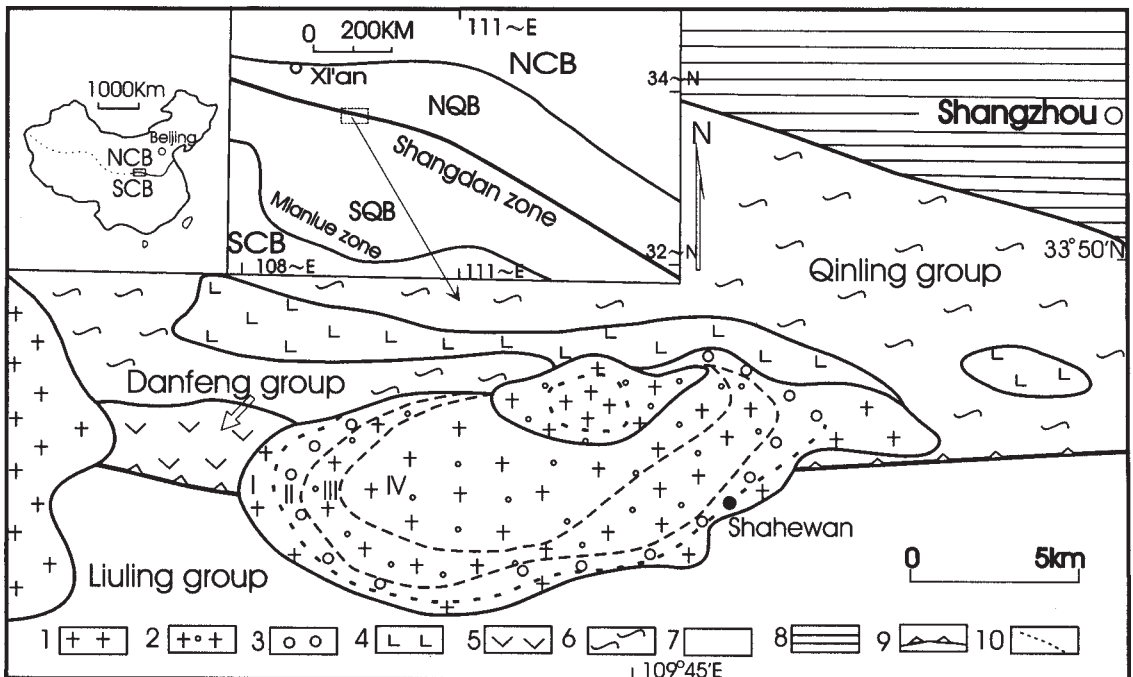


Fig. 1. Geological map showing the regional setting and zonal structure of the Shahewan pluton. Legend: 1. monzogranite; 2. quartz monzonite; 3. rapakivi-textured granite; 4. Lajimiao gabbro; 5. Danfeng group; 6. Qinling group; 7. Liuling group; 8. Cretaceous-Quaternary; 9. Shangdan suture; 10. boundary of petrographic zone. NCB = North China Block, SCB = South China Block; NQB = North Qinling Block; SQB = South Qinling Block. I, II, III and IV show the distribution of the four zonally arranged main rock types discussed in this study.

Leitch et al. 1995, Lu et al. 2000). The Phanerozoic felsic intrusions are of two main age groups: 345 to 380 Ma and 206 to 220 Ma, and many of them are centered on the Shangdan suture (Meng & Zhang 1999). Another suture zone, the Mianlue suture, occurs 100–200 km south of the Shangdan suture. By combining various geological, paleomagnetic and geochronological data, Meng and Zhang (1999) constructed a geotectonic model that involved two orogenic episodes in formation of the Qinling belt. Following a middle Paleozoic subduction and collision along the Shangdan suture, rifting in the southern part of the Qinling belt led to opening of an ocean. Closure of this Paleo-Tethyan Qinling Ocean led to Triassic collision along the Mianlue suture and generation of collision-related felsic intrusions largely located along the Shangdan suture. Instead, in a one-orogeny model, the Shahewan pluton and related 206–220 Ma felsic intrusions are regarded as late post-collisional (perhaps even anorogenic) intrusions (see Lu 1996). In the two-orogeny model they could be interpreted as magmatic arc or collision-related rocks – a possibility that needs further studies.

The Shahewan pluton

The Shahewan pluton is a typical representative of the 206–220 Ma rapakivi-textured intrusions in the Shangdan suture (Fig. 1). To the north, the pluton is in contact with the Proterozoic Qinling group, Proterozoic - Paleozoic Danfeng group and Caledonian Lajimiao gabbro (402.6 ± 17.4 Ma Sm-Nd mineral isochron, Li et al. 1989), which all belong to the North China Block. The Qinling group with amphibolite-facies metamorphism is assumed to form the old Precambrian crystalline basement of the belt (Zhang et al. 1989, Wang et al. 1997), and the Danfeng group consists predominantly of arc volcanic rocks and some possible ophiolite suites. To the south the pluton is in contact with a sandy slate of the Devonian Liuling group. The granite pluton has sharp contact with its wall rocks and has caused contact metamorphism in the Liuling group, forming a hornfels zone 300–1000 m in width. It is ellipsoidal in

shape, trends east-west and has an area of 104 km². Enclaves, consisting of fine-grained hornblende diorite and biotite-hornblende quartz diorite, are frequent in the pluton, particularly at the margins. In some of them, alkali feldspar megacrysts, with or without plagioclase mantle, can be observed.

Three ages have been determined for the Shahewan pluton by various methods: 212.1 ± 1.8 Ma by U-Pb on zircon, 213.9 ± 0.5 Ma by Rb-Sr on whole rock, alkali feldspar, apatite and biotite (MSWD=0.17, $I_{Sr} = 0.705$), and 213.2 ± 2 Ma by Ar-Ar on biotite (Lu et al. 1999, Zhang et al. 1999). These ages are consistent with the regional geology. For example, the pluton has been re-worked neither by late Paleozoic metamorphism (450–350 Ma, You & Suo 1991) nor deformation along the major suture, although many Paleozoic plutons in the suture have been deformed.

PETROGRAPHY

The Shahewan pluton consists of four zonally arranged main rock types (Fig. 1): 1) porphyritic biotite-hornblende monzogranite with about 25 vol% megacrysts, 2) porphyritic biotite-hornblende quartz monzonite with about 10 vol% megacrysts, 3) megacryst-bearing biotite-hornblende quartz monzonite, and 4) medium to coarse-grained porphyritic biotite-hornblende quartz monzonite.

Porphyritic biotite-hornblende monzogranite (with 35–30 vol% plagioclase, 20–25 vol% alkali feldspar, 20–25 vol% quartz, 5–7 vol% biotite, and about 7 vol% hornblende) constitutes the outermost zone of the pluton, especially along its southern margin (Fig. 1). It is light red and has a porphyritic texture with about 25 vol% alkali feldspar megacrysts (Fig. 2). The megacrysts are euhedral or ovoidal in shape and about 2 cm x 4 cm in size. Alkali feldspar in the matrix is anhedral. Hornblende, biotite, plagioclase, and quartz are present as inclusions in the alkali feldspar megacrysts and in the matrix.

Porphyritic biotite-hornblende quartz monzonite (with 25–30 vol% plagioclase, 25–30 vol% alka-

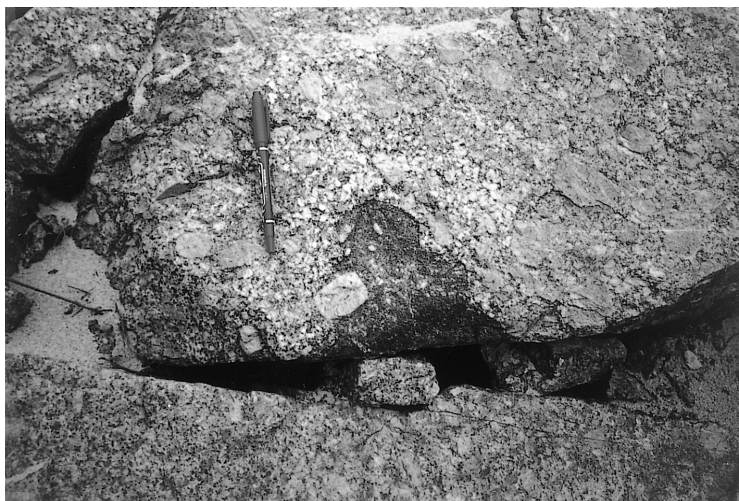


Fig. 2. Porphyritic biotite-hornblende monzogranite in the first, outermost zone of the Shahewan pluton.



Fig. 3. Porphyritic biotite-hornblende quartz monzonite in the second zone of the Shahewan pluton.



Fig. 4. Megacryst-bearing biotite-hornblende quartz monzonite in the third zone of the Shahewan pluton.

Table. 1 Chemical compositions of quartz monzonites from the Shahewan pluton; data from Lu et al. (1996). S1 is from the fourth zone of the Shahewan pluton, S7 from the third zone, and S5 from the second zone. Oxides in wt%, trace elements in ppm.

| Sample | SiO ₂ | TiO ₂ | Al ₂ O ₃ | Fe ₂ O ₃ | FeO | MnO | MgO | CaO | Na ₂ O | K ₂ O | P ₂ O ₅ | H ₂ O ⁺ |
|--------|------------------|------------------|--------------------------------|--------------------------------|------|-------|------|------|-------------------|------------------|-------------------------------|-------------------------------|
| S1 | 67.00 | 0.62 | 14.02 | 1.00 | 2.38 | 0.114 | 2.04 | 2.62 | 4.13 | 4.08 | 0.30 | 0.48 |
| S7 | 64.18 | 0.68 | 15.28 | 1.18 | 2.52 | 0.106 | 2.16 | 3.08 | 4.18 | 4.51 | 0.27 | 1.10 |
| S5 | 65.38 | 0.68 | 14.63 | 1.33 | 2.37 | 0.116 | 2.15 | 2.94 | 4.24 | 4.14 | 0.29 | 0.80 |

| Sample | Ga | Sr | Rb | Nb | Ta | Zr | Hf | Th | F |
|--------|----|-----|-----|------|-----|-----|-----|------|-----|
| S1 | 13 | 360 | 88 | 12.3 | 0.8 | 240 | 7.9 | 17.1 | 510 |
| S7 | 10 | 460 | 101 | 11.3 | 0.8 | 180 | 6.4 | 11.2 | 490 |
| S5 | 12 | 430 | 100 | 13.8 | 1.2 | 190 | 6.4 | 14.0 | 570 |

| Sample | La | Ce | Nd | Sm | Eu | Gd | Yb | Lu | Y | Eu/Eu* |
|--------|-------|-------|-------|------|------|------|------|------|-------|--------|
| S1 | 49.40 | 74.60 | 27.50 | 5.68 | 1.29 | 3.67 | 1.29 | 0.19 | 11.4 | 0.94 |
| S7 | 42.30 | 77.40 | 30.20 | 6.26 | 1.42 | 4.20 | 1.25 | 0.10 | 13.80 | 0.81 |
| S5 | 50.40 | 94.70 | 32.90 | 6.94 | 1.39 | 4.32 | 1.36 | 0.21 | 14.30 | 0.80 |

li feldspar, 10–15 vol% quartz, 5 vol% biotite, and 7–13 vol% hornblende) occurs in the second zone of the pluton and shows roundish or euhedral alkali feldspar megacryst totalling about 10 vol% (Fig. 3), many of them have plagioclase mantles.

The alkali feldspar megacrysts contain commonly one plagioclase mantle, but some have two or three mantles. The mineral composition and texture of the matrix is similar to that in the porphyritic biotite-hornblende monzogranite.

Megacryst-bearing biotite-hornblende quartz monzonite composes the third zone of the pluton. The mineral contents are similar to the second zone except have less than 5 vol% megacrysts (Fig. 4). Some of the alkali feldspar megacrysts are mantled by plagioclase. The minerals in the groundmass of this rock type are the same as those in the first and second zones.

Medium to coarse-grained porphyritic biotite-hornblende quartz monzonite occurs in the fourth zone and is the major rock type of the central part of the pluton. It shows megacrysts of plagioclase and alkali feldspar. Biotite, hornblende, plagioclase, quartz, and alkali feldspar occur in the groundmass. Some of the alkali feldspars have plagioclase mantles.

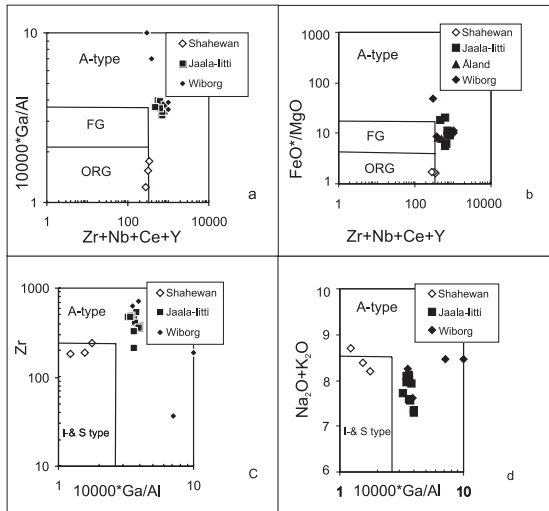


Fig. 5. Geochemical discrimination diagrams after Whalen et al. (1987) adopted to the analyses of the Shahewan, Jaala-Iitti, Åland and Wiborg complexes. a) $10000 \cdot \text{Ga}/\text{Al}$ vs. $(\text{Zr}+\text{Nb}+\text{Ce}+\text{Y})$, b) FeO^*/MgO vs. $(\text{Zr}+\text{Nb}+\text{Ce}+\text{Y})$, c) Zr vs. $10000 \cdot \text{Ga}/\text{Al}$, d) $(\text{Na}_2\text{O}+\text{K}_2\text{O})$ vs. $10000 \cdot \text{Ga}/\text{Al}$. Analyses from Finnish rapakivi granites from Vormaa (1976), Rämö and Haapala (1995), and Salonsaari (1995).

GEOCHEMISTRY

Chemical analyses of the rocks of the Shahewan pluton are presented in Table 1. The rocks are metaluminous with A/CNK around 0.9. Compared with the typical rapakivi granites of Finland (see Vormaa 1976, Rämö & Haapala 1995), the rocks

Table 2. Chemical compositions of hornblendes from the Shahewan pluton (1–6) compared to hornblendes of the Shachang rapakivi granite (7–9; Yu et al. 1996). 1, hornblende of the first generation in the biotite-hornblende quartz monzonite; 2–4, hornblende of the second generation in the biotite-hornblende quartz monzonite; 5–6, hornblende of the enclaves in the Shahewan pluton. Analytical methods: 3–4, wet chemical analyses (Yan 1985); 1, 2, 5 and 6, JCSA-733 microprobe analyses at the Xi'an Geological Institute.

| Sample | 1 | 2 | 3 | 4 | 5 | 6 | 7 | 8 | 9 |
|--------------------------------|--------|--------|--------|--------|--------|--------|--------|--------|--------|
| SiO ₂ | 48.18 | 50.58 | 50.22 | 50.08 | 48.21 | 47.87 | 41.31 | 41.67 | 41.98 |
| TiO ₂ | 0.91 | 0.57 | 0.82 | 0.89 | 1.05 | 0.69 | 1.76 | 1.66 | 1.55 |
| Al ₂ O ₃ | 6.24 | 4.90 | 5.08 | 4.98 | 5.90 | 5.37 | 7.79 | 7.69 | 8.10 |
| Fe ₂ O ₃ | | | 4.58 | 4.50 | | | | | |
| FeO | | | 9.20 | 9.05 | | | | | |
| FeO ₁ | 14.13 | 13.84 | | | 13.06 | 14.31 | 26.22 | 26.98 | 26.97 |
| MnO | 0.04 | 0.38 | 0.43 | 0.41 | 0.32 | 0.37 | 0.58 | 0.68 | 0.43 |
| MgO | 13.62 | 15.29 | 14.95 | 15.05 | 14.27 | 13.90 | 4.14 | 4.15 | 4.49 |
| CaO | 10.30 | 10.41 | 12.17 | 12.14 | 11.11 | 11.63 | 10.01 | 10.30 | 10.32 |
| Na ₂ O | 1.41 | 1.21 | 1.15 | 1.14 | 2.41 | 0.89 | 1.69 | 2.09 | 1.82 |
| K ₂ O | 0.54 | 0.12 | 0.50 | 0.38 | 0.18 | 0.30 | 1.59 | 1.47 | 1.42 |
| NiO | 0.03 | 0.00 | | | 0.00 | 0.00 | 0.00 | 0.07 | 0.00 |
| Cr ₂ O ₃ | 0.11 | 0.03 | | | 0.00 | 0.08 | 0.00 | 0.00 | 0.00 |
| P ₂ O ₅ | 0.26 | 0.28 | | | 0.00 | | 0.00 | 0.10 | 0.37 |
| Total | 95.51 | 97.33 | 99.10 | 98.62 | 95.34 | 95.41 | 95.08 | 96.86 | 97.45 |
| Si | 7.1340 | 7.3114 | 7.1900 | 7.1969 | 7.0847 | 7.1377 | 6.6322 | 6.6080 | 6.5946 |
| Al | 0.8660 | 0.6886 | 0.8100 | 0.8031 | 0.9153 | 0.8623 | 1.3678 | 1.3920 | 1.4054 |
| Total | 8.0000 | 8.0000 | 8.0000 | 8.0000 | 8.0000 | 8.0000 | 8.0000 | 8.0000 | 8.0000 |
| Al | 0.2231 | 0.1462 | 0.0469 | 0.0406 | 0.1073 | 0.0821 | 0.1062 | 0.0449 | 0.0946 |
| Fe ³⁺ | 0.5178 | 0.4967 | 0.4938 | 0.4870 | 0.4768 | 0.5376 | 0.9290 | 0.9328 | 0.9251 |
| Ti | 0.1014 | 0.0617 | 0.0890 | 0.0959 | 0.1157 | 0.0771 | 0.2122 | 0.1982 | 0.1831 |
| Mg | 3.0056 | 3.2939 | 3.1902 | 3.2237 | 3.1251 | 3.0886 | 0.9907 | 0.8905 | 1.0516 |
| Fe ²⁺ | 1.1721 | 1.0015 | 1.1013 | 1.0881 | 0.0756 | 1.1962 | 2.1879 | 2.5413 | 2.5157 |
| Mn | | | 0.0525 | 0.0500 | 0.0400 | 0.0184 | 0.0791 | 0.0915 | 0.0576 |
| Total | 5.0000 | 5.0000 | 4.9737 | 4.9853 | 4.9405 | 5.0000 | 4.8051 | 4.7892 | 4.8277 |
| Fe ²⁺ | 0.0206 | 0.1191 | | | | 0.0282 | | | |
| Mn | 0.0053 | 0.0469 | | | | | | | |
| Ca | 1.6345 | 1.6122 | 1.8670 | 1.8696 | 1.7493 | 1.8583 | 1.7220 | 1.7504 | 1.7369 |
| Na | 0.3396 | 0.2218 | 0.1330 | 0.1304 | 0.2507 | 0.1135 | 0.2780 | 0.2496 | 0.2631 |
| Total | 2.0000 | 2.0000 | 2.0000 | 2.0000 | 2.0000 | 2.0000 | 2.0000 | 2.0000 | 2.0000 |
| Na | 0.0643 | 0.1170 | 0.1871 | 0.1762 | 0.4363 | 0.1446 | 0.2478 | 0.3926 | 0.2910 |
| K | 0.0104 | 0.0226 | 0.0912 | 0.0691 | 0.0336 | 0.0573 | 0.3261 | 0.2973 | 0.2850 |
| Fe/(Fe+Mg) | 0.36 | 0.33 | 0.33 | 0.33 | 0.15 | 0.36 | 0.78 | 0.78 | 0.77 |
| Mg/(Mg+Fe ²⁺) | 0.72 | 0.77 | 0.68 | 0.75 | 0.98 | 0.72 | 0.31 | 0.26 | 0.29 |

are low in Si, K, F, Ga, Zr, Y, Fe/Mg, and K/Na (Table 1, Fig. 5). They straddle the boundary of A-type granite and ORG (ocean ridge granites) fields (Fig. 5a, b) and the fields of A-type granite and I & S type granites (Fig. 5c, d). Negative Eu

anomaly, which is characteristic for the typical rapakivi granites, does not occur in the Shahewan rocks that have Eu/Eu* values from 0.8 to 0.94.

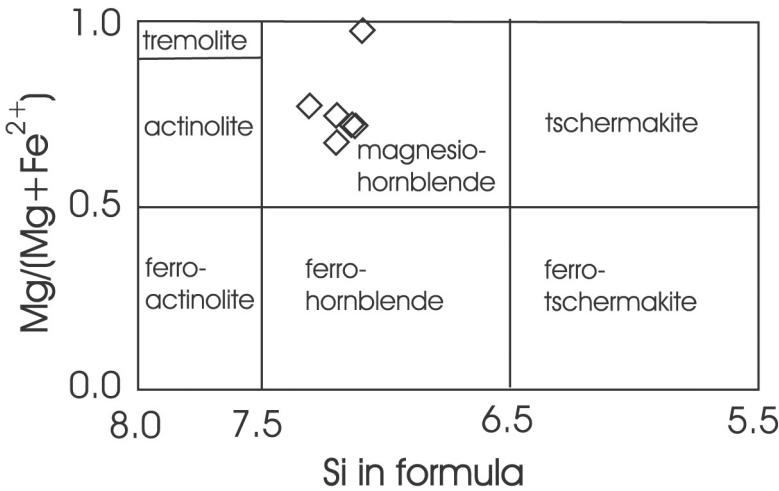


Fig. 6. Classification of calcic amphiboles with $(Na+K)_A \geq 0.50$ (after Leake et al. 1997), and compositions of amphiboles from the Shahewan pluton.

MINERALOGY

There are three mineral assemblages in the four main rock types of the Shahewan pluton. The first includes early biotite + hornblende + plagioclase + quartz, occurring as inclusions in the alkali feldspar megacrysts. The second assemblage consists of euhedral or ovoidal alkali feldspar megacrysts that occur together with plagioclase megacrysts, and the third assemblage of biotite + hornblende + plagioclase + alkali feldspar + quartz in the groundmass. The accessory minerals are Fe-Ti oxide, titanite, apatite, zircon, rutile, and fluorite.

Hornblende

Hornblende is the main Fe-Mg silicate in the pluton. It occurs in two generations, as inclusions in the alkali feldspar megacrysts and in the groundmass. The hornblende inclusions (less than 1 vol%) in the megacrysts are green to yellowish green. The hornblende in the matrix is euhedral to subhedral with grain size of 0.6 mm x 1.5 mm to 2 mm x 3.5 mm and bluish green to yellowish green in color. This kind of hornblende accounts for 7–13 vol% and contains titanite, apatite, and Fe-Ti oxide as inclusions.

The hornblende diorite enclaves contain hornblende aggregates that account for 15–20 vol%.

Most of the hornblende grains in the aggregates are zoned with dark green margins and light green cores. Inclusions in them are titanite, apatite, Fe-Ti oxide, and occasional quartz.

Wet chemical (Yan 1985) and electron microprobe analyses of the hornblendes are given in Table 2. The wet chemical analyses were calculated to 24 oxygen atoms and the microprobe analyses to 23 oxygen atoms. The Fe^{2+}/Fe^{3+} ratio was calculated from wet chemical analyses.

From the early generation to the later, the content of SiO_2 in hornblende increases, but K_2O and Al_2O_3 decrease. The hornblende of the enclaves has composition close to those in the host rocks. This may suggest that chemical equilibrium was reached between the enclaves and the surrounding magma. According to the amphibole classification of Leake et al. (1997), all the hornblendes are calcic amphiboles and plot in the magnesiohornblende field (Fig. 6). The $Mg/(Mg+Fe^{2+})$ and $Fe/(Fe+Mg)$ are 0.68–0.98 and 0.15–0.36, respectively, showing that the hornblendes are rich in Mg and poor in Fe. Hornblende of the later generation has lower Ti content than hornblende of the earlier generation and enclaves (Table 2). The Ti content of calcic hornblende is not affected by pressure, but it increases with increasing temperature and with decreasing oxygen fugacity (see Spear et al. 1981).

The amphibole geothermometer of Helz et al. (1979) gives crystallization temperature of 937°C for the hornblende of the enclaves, 859°C for the early hornblende generation, and 759°C for the later generation.

Biotite

Biotite has two generations in the Shahewan pluton. The first generation biotite occurs as very

small inclusions in the megacrysts and its contents is less than 0.5 vol%. Biotite of the second generation occurs as euhedral to subhedral grains in the groundmass. It is dark brown to light brown and accounts for about 5 vol%. Some biotite grains are partly replaced by chlorite. Titanite, apatite, and Fe-Ti oxide occur as inclusions in the second generation.

Wet chemical and microprobe analyses of biotite of the second generation are listed in Table

Table 3. Chemical compositions of biotites from the Shahewan pluton (1-6), compared to the biotites of the Shachang rapakivi granite (7-8; Yu et al. 1996). The analyses: 1-6, biotite of the second generation in the biotite-hornblende quartz monzonite. The analytical methods; 3-6, wet chemical analyses (Yan 1985); 1-2, JCSA-733 microprobe analyses at Xi'an geological Institute.

| Sample | 1 | 2 | 3 | 4 | 5 | 6 | 7 | 8 |
|--------------------------------|--------|--------|--------|--------|--------|--------|--------|--------|
| SiO ₂ | 37.90 | 38.40 | 34.83 | 36.20 | 36.83 | 36.50 | 36.33 | 35.52 |
| TiO ₂ | 2.89 | 2.66 | 3.20 | 2.80 | 2.80 | 2.70 | 3.24 | 3.2 |
| Al ₂ O ₃ | 13.41 | 14.10 | 13.15 | 13.67 | 12.87 | 13.44 | 12.35 | 13.63 |
| Fe ₂ O ₃ | | | 4.46 | 5.38 | 4.00 | 4.78 | | |
| FeO | | | 14.78 | 13.42 | 14.60 | 13.87 | | |
| FeO _t | 17.76 | 17.59 | | | | | 28.83 | 29.52 |
| MnO | 0.12 | 0.19 | 0.27 | 0.42 | 0.32 | 0.30 | 0.64 | 0.54 |
| MgO | 13.94 | 14.56 | 14.61 | 15.33 | 14.25 | 14.46 | 4.65 | 3.45 |
| CaO | 0.13 | 0.03 | 2.00 | 1.57 | 1.08 | 1.50 | 0.09 | 0.06 |
| Na ₂ O | 0.18 | 0.05 | 0.35 | 0.30 | 0.28 | 0.20 | 0.3 | 0.1 |
| K ₂ O | 8.89 | 8.48 | 5.30 | 5.80 | 8.20 | 7.96 | 9.02 | 9.17 |
| P ₂ O ₅ | | | | | | | | |
| H ₂ O | | | 6.54 | 4.96 | 4.86 | 4.18 | | |
| H ₂ O | | | | | | | | |
| Total | 95.20 | 96.06 | 99.49 | 99.85 | 99.86 | 99.65 | 95.45 | 95.19 |
| Si | 2.8400 | 2.7684 | 2.6954 | 2.6152 | 2.8336 | 2.7965 | 2.8152 | 2.7684 |
| Al | 1.1600 | 1.1957 | 1.1983 | 1.1975 | 1.1664 | 1.2035 | 1.1282 | 1.2316 |
| Ti | | 0.0359 | 0.1063 | 0.1562 | | | 0.0566 | |
| Fe ³⁺ | | | | 0.0311 | | | | |
| Total | 4.0000 | 4.0000 | 4.0000 | 4.0000 | 4.0000 | 4.0000 | 4.0000 | 4.0000 |
| Al | 0.0190 | | | | 0.0010 | 0.0106 | | 0.0208 |
| Ti | 0.1579 | 0.1070 | 0.0797 | | 0.1618 | 0.1556 | 0.1322 | 0.1876 |
| Fe ³⁺ | 0.3240 | 0.3119 | 0.2595 | 0.2699 | 0.2316 | 0.2758 | 0.9686 | 0.9789 |
| Fe ²⁺ | 0.7515 | 0.7192 | 0.9566 | 0.8340 | 0.9394 | 0.8886 | 0.7919 | 0.8363 |
| Mn | 0.0045 | 0.0134 | 0.0177 | 0.0263 | 0.0208 | 0.0193 | 0.0420 | 0.0357 |
| Mg | 1.5525 | 1.5597 | 1.6849 | 1.6976 | 1.6454 | 1.6510 | 0.5370 | 0.4007 |
| Total | 2.8094 | 2.7112 | 2.9984 | 2.8278 | 3.0000 | 3.0000 | 2.4717 | 2.4600 |
| Ca | 0.0090 | 0.0217 | 0.1660 | 0.1250 | 0.0872 | 0.1229 | 0.0075 | 0.0050 |
| Na | 0.0270 | 0.0433 | 0.0529 | 0.0433 | 0.0416 | 0.0387 | 0.0451 | 0.0151 |
| K | 0.8370 | 0.7711 | 0.5236 | 0.5496 | 0.8049 | 0.7287 | 0.8917 | 0.9118 |
| Total | 0.8730 | 0.8361 | 0.7429 | 0.7179 | 0.9337 | 0.8903 | 0.9443 | 0.9319 |
| OH | | | 3.3600 | 2.4580 | 2.3856 | 1.9900 | | |
| F | | | | | | | | |
| Fe/(Fe+Mg) | 0.40 | 0.40 | 0.42 | 0.40 | 0.42 | 0.41 | 0.77 | 0.82 |
| Mg/(Mg+Fe ²⁺) | 0.67 | 0.68 | 0.64 | 0.67 | 0.64 | 0.65 | 0.40 | 0.32 |

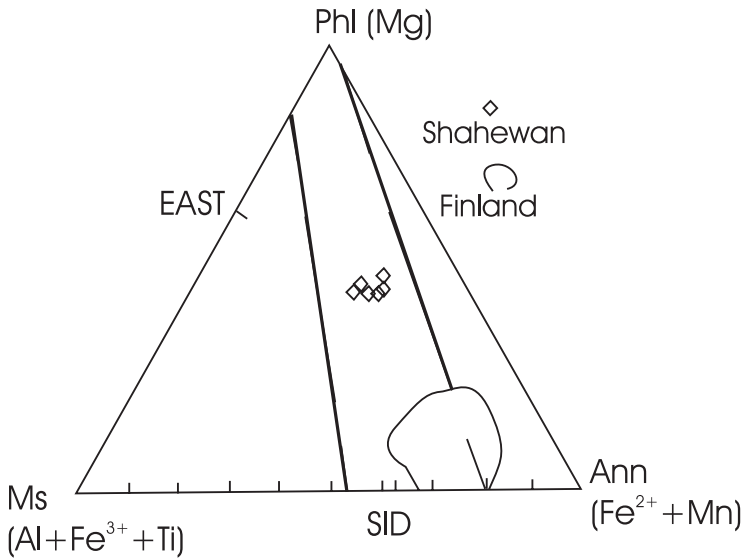


Fig. 7. Classification of biotites (after Forster 1960). The field of biotite from the Finnish rapakivi granites (Rieder et al. 1996).

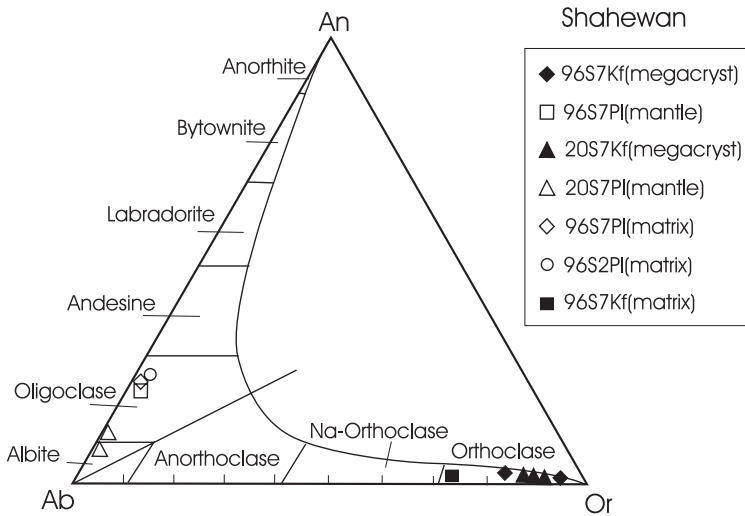


Fig. 8. Classification of feldspars.

3. The wet chemical analyses are calculated to 12 and the microprobe analyses to 11 oxygen atoms. The Fe^{2+}/Fe^{3+} ratios of the microprobe analyses were estimated from wet chemical analyses. According to the terminology of Foster (1960), the biotites belong to Mg-biotites (Fig. 7) with $Fe/(Fe+Mg)$ of 0.40–0.42 and $Mg/(Mg+Fe^{2+})$ of 0.64–0.68. The equilibrium temperature for biotite and hornblende of the second generation is 750–820°C (Wang & Lu 1998).

Plagioclase

Plagioclase occurs in two generations: as inclusions in alkali feldspar megacrysts and, more abundantly, in the groundmass. Some plagioclase is also found as mantles on alkali feldspar megacrysts. The plagioclase inclusions are partly sericitized, euhedral, and measure 0.25 mm x 0.5 mm to 0.3 mm x 0.7 mm. Most of them have water-clear albite margin and the fresh grains are oligoclase with An about 25 mole%. In the ground-

Table 4. Electron microprobe analyses of alkali feldspars (Kf) and plagioclases (Pl). Analyses by a JXA-733 microprobe at the Xi'an Geological Institute .

| Sample | mineral | SiO ₂ | TiO ₂ | Al ₂ O ₃ | Cr ₂ O ₃ | FeO _t | MnO | MgO | NiO |
|--------|------------|------------------|------------------|--------------------------------|--------------------------------|------------------|------|------|------|
| 96S7 | Kf(core) | 64.15 | 0.00 | 18.72 | 0.00 | 0.21 | 0.00 | 0.00 | 0.09 |
| 96S7 | Kf(margin) | 64.28 | 0.02 | 19.82 | 0.02 | 0.13 | 0.00 | 0.00 | 0.00 |
| 96S7 | Pl(mantle) | 61.71 | 0.06 | 24.90 | 0.08 | 0.15 | 0.00 | 0.03 | 0.09 |
| 20S7 | Kf(core) | 64.19 | 0.06 | 18.85 | 0.00 | 0.47 | 0.07 | 0.08 | 0.00 |
| 20S7 | Kf(middle) | 63.99 | 0.00 | 19.38 | 0.00 | 0.29 | 0.00 | 0.11 | 0.00 |
| 20S7 | Kf(margin) | 66.64 | 0.03 | 18.38 | 0.00 | 0.19 | 0.00 | 0.00 | 0.04 |
| 20S7 | Pl(mantle) | 67.98 | 0.02 | 20.49 | 0.06 | 0.15 | 0.00 | 0.03 | 0.00 |
| 20S7 | Pl(mantle) | 66.45 | 0.03 | 21.85 | 0.23 | 0.00 | 0.01 | 0.09 | 0.02 |
| 96S7 | Pl(matrix) | 62.13 | 0.00 | 24.97 | 0.08 | 0.23 | 0.00 | 0.04 | 0.00 |
| 96S2 | Pl(matrix) | 63.46 | 0.00 | 24.32 | 0.00 | 0.22 | 0.06 | 0.02 | 0.06 |
| 96S7 | Kf(matrix) | 66.71 | 0.02 | 19.48 | 0.05 | 0.07 | 0.00 | 0.00 | 0.00 |

| Sample | mineral | CaO | Na ₂ O | K ₂ O | Total | An | Ab | Or |
|--------|------------|------|-------------------|------------------|--------|-------|-------|-------|
| 96S7 | Kf(core) | 0.05 | 0.49 | 15.93 | 99.64 | 0.20 | 4.50 | 95.30 |
| 96S7 | Kf(margin) | 0.33 | 1.54 | 13.63 | 99.77 | 1.80 | 14.30 | 83.90 |
| 96S7 | Pl(mantle) | 4.25 | 8.37 | 0.41 | 100.4 | 21.3 | 76.20 | 2.50 |
| 20S7 | Kf(core) | 0.01 | 0.72 | 15.23 | 99.68 | 0.10 | 6.70 | 93.20 |
| 20S7 | Kf(middle) | 0.19 | 1.07 | 14.92 | 99.99 | 0.90 | 9.80 | 89.30 |
| 20S7 | Kf(margin) | 0.04 | 1.35 | 13.96 | 100.62 | 1.30 | 12.80 | 86.90 |
| 20S7 | Pl(mantle) | 1.59 | 9.64 | 0.08 | 100.06 | 8.50 | 91.00 | 0.50 |
| 20S7 | Pl(mantle) | 2.36 | 9.43 | 0.01 | 100.48 | 12.10 | 87.80 | 0.01 |
| 96S7 | Pl(matrix) | 4.49 | 8.17 | 0.33 | 100.43 | 22.80 | 75.20 | 2.00 |
| 96S2 | Pl(matrix) | 4.52 | 7.20 | 0.48 | 100.27 | 25.00 | 72.10 | 2.90 |
| 96S7 | Kf(matrix) | 0.13 | 2.48 | 11.07 | 100.00 | 0.80 | 25.20 | 74.00 |

mass, plagioclase grains are subhedral and show albite twinning or combination of Carlsbad and albite twins, as well as zoning. Electron microprobe analyses and numerous optical determinations show the An of central part of fresh grains to be 28–32 mole% and at the margin 22–25 mole%. The plagioclase mantle consists of differently orientated plagioclase grains with An about 8–21 mole% (Table 4; Fig. 8).

Alkali feldspar

Alkali feldspar is present as megacrysts and in the groundmass. The megacrysts are both ovoidal and euhedral in shape, and their diameter is mostly from 3 cm to 5 cm, in exceptional cases up to 16 cm. The alkali feldspar megacrysts show Carlsbad twinning and perthitic texture. Some of the megacrysts are surrounded by one or, occasionally, two or three oligoclase mantles, measuring from 1 mm to 2 mm in thickness (Figs. 9, 10). Both the

plagioclase mantle and alkali feldspar megacrysts have inclusions of quartz, Fe-Ti oxide, plagioclase, hornblende, and biotite. The perthitic texture is not as pronounced in the groundmass alkali feldspars as in the megacrysts. The contents of Al₂O₃, CaO, and Na₂O increase and K₂O decrease from the core of the alkali feldspar megacrysts to their margins and farther to the groundmass alkali feldspar. The Or content is about 95 mole% in the core of the alkali feldspar megacrysts and 84 mole% at the margin. The groundmass alkali feldspar has 74 mole% Or (Table 4).

Quartz

Quartz also occurs in two generations: as concave and drop-like inclusions in the alkali feldspar megacrysts and as anhedral grains in the groundmass (10–20 vol%). The quartz inclusions are not more than 0.2 mm in diameter. The groundmass quartz is anhedral, measuring mostly from 0.4 mm

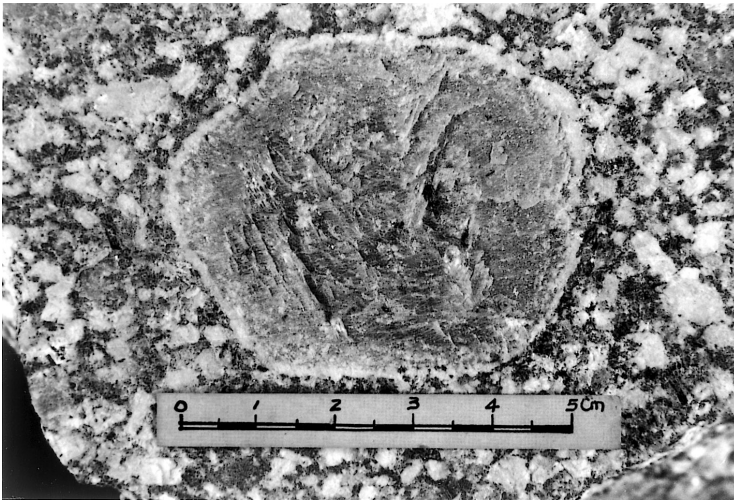


Fig. 9. Rapakivi texture, sub-ovoidal alkali-feldspar megacryst with one plagioclase mantle. Both the core and the mantle have inclusions of hornblende, biotite, plagioclase, and quartz.

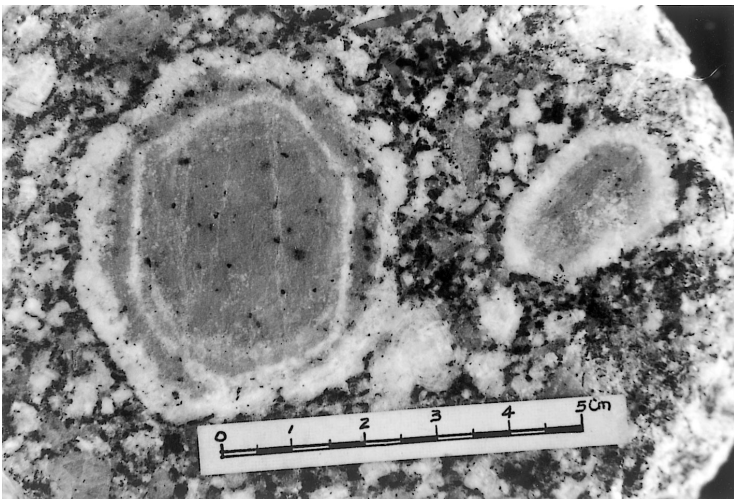


Fig. 10. Rapakivi texture, euhedral alkali feldspar megacryst with two plagioclase mantles. Inclusions become more abundant at the margins of the megacryst.

to 3 mm in diameter. Euhedral large quartz grains, such as in the typical rapakivi granites of Finland (e.g. Vorma, 1971, 1976), are rare in the Shahewan pluton.

Discussion and conclusions

The classical rapakivi granites of Fennoscandia are characterized by textural, mineralogical and geochemical features that separate them from many other granites. According to Vorma (1976), the rapakivi texture *sensu stricto* is characterized by

- 1) ovoidal shape of the alkali feldspar megacrysts,
- 2) mantling of part of the ovoids by plagioclase shells, and
- 3) presence of two generations of alkali feldspar and quartz, the idiomorphic, older quartz having crystallized as high quartz. Rapakivi texture *sensu lato* involves only the presence of mantled alkali feldspar ovoids. Emphasizing the textural, geochemical and mineralogical characteristics, Haapala and Rämö (1992) redefined the rapakivi granites as “A-type granites characterized by the presence, at least in the larger batholiths, of granite varieties showing the rapakivi texture”.

Rapakivi granites are generally Proterozoic, 1.8 to 1.0 Ga in age, but also Archean and Phanerozoic examples are known (Rämö & Haapala 1995, 1996, Haapala & Rämö 1999). They are generally intracratonic, and mafic underplating, including melting of the deep crust by mantle-derived magmas, is regarded as a possible genetic model (e.g. Bridgwater et al. 1974, Emslie 1978, Haapala & Rämö 1990, Rämö & Haapala 1996). However, Wernick et al. (1997) have described a 0.59 Ga arc-related rapakivi granite suite from the Itu Province in southwestern Brazil that overlaps or shortly follows the synorogenic calc-alkaline Brazilian magmatism.

In chemical composition, the rocks of the Shahewan pluton are lower in Si, K, F, Ga, Zr, Y, LREE, Fe/Mg, and K/Na (Table 1) than classical rapakivi granites. In the discrimination diagrams (Fig. 5), the Shahewan rocks and the classical rapakivi granites are located in different fields. The classical rapakivi granites are A-type granites, but the rocks of the Shahewan straddle on the boundary of A-type granite field. Thus, the chemical composition of the rocks also suggests that the Shahewan pluton is not A-type granite. In addition, the REE patterns with Eu/Eu* from 0.8 to 0.94 (Table 1) differ from those of typical rapakivi granites (see Vorma 1976, Rämö & Haapala 1995, 1996).

The mafic minerals (biotite, hornblende, and fayalite) of typical rapakivi granites are characterized by a very high Fe content. In the rapakivi granites of Finland, the Fe/(Fe+Mg) value ranges from 0.77 to 0.99 in hornblende and from 0.82 to 1.00 in biotite (Simonen & Vorma 1969, Haapala 1977, Salonsaari 1995, Rieder et al. 1996). Hornblende and biotite of the Shachang rapakivi granite in China also exhibit high Fe/(Fe+Mg), 0.70–0.78 for hornblende and 0.76–0.92 for biotite (Yu et al. 1996). The mafic minerals in the Shahewan pluton, however, have much lower Fe/(Fe+Mg) values, 0.33–0.36 for hornblende and 0.40–0.42 for biotite.

The compositions of hornblende and biotite in granitoid rocks reflect the whole rock composition and the origin of the granitoid. The Fe-enriched mafic minerals are a typical feature of A-type

granitoids (Eby 1990, Fattach & Rahman 1994). The mafic minerals, biotite and hornblende, of the Shahewan pluton are poor in Fe but rich in Mg (Wang & Lu 1998). On the basis of the mafic mineral compositions, the Shahewan pluton is not A-type granite. However, its whole rock geochemistry shows some features transitional between I- and A-type granites.

The occurrence of oligoclase-mantled alkali feldspar megacrysts in the Shahewan pluton is a feature typical of rapakivi granites and justifies to use the term rapakivi texture *sensu lato* (see Vorma 1976). Other textural features are equivocal. Euhedral quartz crystals are found only locally in the matrix. The relatively late crystallization of quartz is obviously related to the low silica content of the Shahewan granite - quartz monzonite magma (the rocks contain 65 to 68 wt% SiO₂). Inclusions of plagioclase, hornblende, biotite, and quartz in the alkali feldspar megacrysts are common in both the Shahewan pluton and classical rapakivi granites, but this feature is not diagnostic of the rapakivi granites.

Taking into account the similarities and different features of the Shahewan granite - quartz monzonite and the classical rapakivi granites, we feel that it is appropriate to regard the Shahewan as a rapakivi-textured granite - quartz monzonite (or as granite - quartz monzonite containing plagioclase-mantled alkali feldspar megacrysts) rather than to include it in true rapakivi granites.

ACKNOWLEDGEMENTS. This work was supported by grant 40072065 from the National Natural Science Foundation of China, the Opening Foundation of the Key Laboratory of Northwest University Continental Dynamics, Ministry of Education, and the Project of the Important Geological Problem on China Granites from Geological Survey of China. We thank professors Zhang Guowei, Hong Dawei, Xiao Qinhui, Mao Jingwen and Zhang Chengli for stimulating discussions about rapakivi granite. We also thank professor Hanna Nekvasil and senior researcher O. Tapani Rämö for a careful review of the manuscript and useful suggestions.

REFERENCES

- Bridgwater, D., Sutton, J. & Watterson, J. 1974. Crustal downfolding associated with igneous activity. *Tectonophysics* 21, 57–77.
- Eby, G.N. 1990. The A-type granitoids: A review of their occurrence and chemical characteristics and speculation on their petrogenesis. *Lithos* 26, 115–134.
- Emslie, R.F. 1978. Anorthosite massifs, rapakivi granites, and Late Proterozoic rifting of North America. *Precambrian Research* 7, 61–98.
- Fattah, A. & Rahman, A. 1994. Nature of biotite from alkaline, calc-alkaline and peraluminous magmas. *Journal of Petrology* 35, 525–532.
- Froster, C.D. 1960. Interpretation of the composition of trioctahedral mica. U.S. Geological Survey, Professional Paper 354-B, 11–49.
- Haapala, I. 1977. Petrography and geochemistry of the Eurajoki stock, a rapakivi-granite complex with greisen-type mineralization in southwestern Finland. *Geological Survey of Finland Bulletin* 286, 89–93.
- Haapala, I. & Rämö, O.T. 1990. Petrogenesis of the Proterozoic rapakivi granites of Finland. In: Stein, H.J. & Hannah, J.L. (eds.) *Ore-bearing Granite Systems: Petrogenesis and Mineralizing Processes*. Geological Society of America, Special Paper 246, 275–286.
- Haapala, I. & Rämö, O.T. 1992. Tectonic setting and origin of the Proterozoic rapakivi granite of southeastern Fennoscandia. *Transactions of the Royal Society of Edinburgh, Earth Sciences* 83, 165–171.
- Haapala, I. & Rämö, O.T. 1999. Rapakivi granite and related rocks: an introduction. *Precambrian Research* 95, 1–7.
- Helz, R.T. 1979. Alkali exchange between hornblende and melt: a temperature-sensitive reaction. *American Mineralogist* 64, 953–965.
- Leake, B.E., Woolley, A.R., Arps, C.E.S., Birch, W.D., Gilbert, M.C., Grice, J.D., Hawthorne, F.C., Kato, A., Kisch, H.J., Krivovichev, V.G., Linthout, K., Laird, J., Mandarino, J., Maresch, W.V., Nickel, E.H., Rock, N.M.S., Schumacher, J.C., Smith, D.C., Stephenson, N.C.N., Ungaretti, L., Whittaker, E.J.W. & Youzhi, G. 1997. Nomenclature of amphibole: report of the Subcommittee on Amphiboles of the International Mineralogical Association Commission on New Minerals and Mineral Names. *Mineralogical Magazine* 61, 295–321.
- Lerch, M.F., Xue, F., Kröner, A., Zhang, G.W. & Tod, W. 1995. A middle Silurian - early Devonian magmatic arc in the Qinling Mountains of Central China. *Journal of Geology* 103, 437–449.
- Li, S.G., Hart, S.R., Zheng, Sh.G., Guo, An.I., Liu, D.I. & Zhang, G.W. 1989. The evidence of Sm-Nd age for the collision of Huabei Plate. *Science in China* 3(B), 312–319 (in Chinese).
- Lu, X.X., Dong Y., Chang, Q.L., Xiao, Q.H., Li, X.B. & Wang, X.X. 1996. Indosinian Shahewan rapakivi granite in Qinling and its dynamic significance. *Science in China* 39, 244–248.
- Lu, X.X., Yu, X.D. & Xiao, Q.H. 1998. The discovery of rapakivi granite in the west Qinling. *Geological Review* 14 (5), 535. (in Chinese with English abstract)
- Lu, X.X., Wei, X.D., Xiao, Q.H., Zhang, Zh.Q., Li, H.M. & Wang, W. 1999. Geochronological studies of rapakivi granites in Qinling and its geological implications. *Geological Journal of China Universities* 15 (4), 372–377. (in Chinese with English abstract)
- Lu, X.X., Xiao, Q.H. & Dong, Y. 2000. Geological map of the granites in the Qinling orogenic belt. Xi'an: Xi'an Map Publishing House. (in Chinese with English abstract)
- Mattauer, M., Matte, P., Malaveille, J., Tapponier, P., Malusci, H., Xu, Zh.Q., Lu, Y.L. & Tang, Y.Q. 1985. Tectonics of the Qinling belt: build-up and evolution of eastern Asian. *Nature* 317, 496–500.
- Meng, Q.R. & Zhang, G.W. 1999. Timing of collision of the North and South China blocks: controversy and reconciliation. *Geology* 27, 123–126.
- Rämö, O.T. & Haapala, I. 1995. One hundred years of rapakivi granite. *Mineralogy and Petrology* 52, 129–146.
- Rämö, O.T. & Haapala, I. 1996. Rapakivi granite magmatism: A global review with emphasis on petrogenesis. In: Demaiffe, D. (ed.) *Petrology and geochemistry of magmatic suites of rocks in the continental and oceanic crusts. A volume dedicated to Professor Jean Michot*. Université Libre de Bruxelles. Royal Museum for Central Africa (Tervuren), 177–200.
- Rieder, M., Haapala, I. & Povondra, P. 1996. Mineralogy of dark mica from the Wiborg rapakivi granite batholith, southeastern Finland. *European Journal of Mineralogy* 8, 593–605.
- Salonsaari, P.T. 1995. Hybridization in the subvolcanic Jaala-Iitti complex and its petrogenetic relation to rapakivi granites and associated mafic rocks of southeastern Finland. *Bulletin of the Geological Society of Finland* 67, Part 1b, 104 p.
- Simonen, A. & Vormaa, A. 1969. Amphibole and biotite from rapakivi granite. *Bulletin de la Commission géologique de Finlande* 238, 5–28.
- Spear, F.S. 1981. An experimental study of hornblende stability and composition variability in amphibolite. *American Journal of Science* 281, 697–734.
- Vormaa, A. 1971. Alkali feldspars of the Wiborg rapakivi massif in southeastern Finland. *Bulletin de la Commission géologique de Finlande* 246, 72 p.
- Vormaa, A. 1976. On the petrochemistry of rapakivi granite with special reference to the Laitila massif, southwestern Finland. *Geological Survey of Finland, Bulletin* 285, 98 p.
- Wang, T., Hu, N.G., Pei, X.Z. & Li, W.P. 1997. The composition structural regime and evolution of the core composition of the Qinling orogenic belt, central China. *Acta Geocientia Sinica* 18, 345–351 (in Chinese with English abstract).

- Wang, X.X. & Lu X.X. 1998. A study of biotite from the Shahewan rapakivi granite in Qinling and its significance. *Acta Petrologica et Mineralogica* 17, 352–358 (in Chinese with English abstract).
- Wernick, E., Galembeck, T.M.B., Godoy, A.M. & Hörmann, P.K. 1995. Geochemical variability of the Rapakivi Itu province, state of São Paulo, SE Brazil. In: Dall’Agnol, R. & Bettencourt, J.S. (eds.) *Proceedings of the Symposium on Rapakivi Granites and Related Rocks, Belem (Brazil)*. August 2–5, 1995. 1997, *Anais da Academia Brasileira de Ciências* 69, 395–413.
- Whalen, A.J.R. & Chappell, B.W. 1987. A-type granites: geochemical characteristics, discrimination and petrogenesis. *Contributions to Mineralogy and Petrology* 95, 407–419.
- Yan, Zh. 1985. Shaanxi Granite. Xi’an Jiaotong University Press. (in Chinese with English abstract)
- You, Z.D. & Suo, S.T. 1991. Metamorphic process and structural analysis of the core complex of an orogenic belt: example from the Eastern Qinling Mountain. China University of Geosciences Press (in Chinese with English abstract).
- Yu, J.H., Fu, H.Q., Zhang, F.L., Wan, F.X., Haapala, I., Rämö, O.T. & Fatisiqi, M. 1996. Anorogenic rapakivi granites and related rocks in northern of the North China Craton, Beijing. Beijing: Science and Technology Press. (in Chinese with English summary on pp. 137–182)
- Zhang, G.W., Yu, Z.P., Sun, Y., Cheng, S.Y., Li, T.H., Xue, F. & Zhang, C.L. 1989. The major suture zone of the Qinling orogenic belt. *Journal of Southeast Asian Earth Sciences* 3, 63–76.
- Zhang, Zh.Q., Zhang, G.W., Tang S.H. & Lu, X.X. 1999. Age of the Shahewan rapakivi granite in Qinling orogen, China and its constraints on the end time of the major orogenic stage of this orogen. *Science in China* 44, 981–983.